



Deep learning algorithm performance evaluation in detection and classification of liver disease using CT images

R. V. Manjunath¹ · Anshul Ghanshala² · Karibasappa Kwadiki³

Received: 19 May 2022 / Revised: 10 August 2022 / Accepted: 22 April 2023 /

Published online: 15 May 2023

© The Author(s), under exclusive licence to Springer Science+Business Media, LLC, part of Springer Nature 2023

Abstract

To diagnose the liver diseases computed tomography images are used. Most of the time even experienced radiologists find it very tough to note the type, size, and severity of the tumor from computed tomography images due to various complexities involved around the liver. In recent years it is very much essential to develop a computer-assisted imaging technique to diagnose liver disease in turn which improves the diagnosis of a doctor. This paper explains a novel deep learning model for detecting a liver disease tumor and its classification. Tumor from computed tomography images has been classified between Metastasis and Cholangiocarcinoma. We demonstrate that our model predominantly performs very well concerning the accuracy, dice similarity coefficient, and specificity parameters compared to well-known existing algorithms, and adapts very well for different datasets. A dice similarity coefficient value of **98.59%** indicates the supremacy of the model.

Keywords Computed tomography · Deep learning · Metastasis · Carcinoma · Cholangiocarcinoma · Labelled images · Unet

1 Introduction

Liver is the largest organ, present below the ribcage on the right side of the belly. Abnormal liver cells growth on or in the liver leads to a lump called liver tumor, which indicates a liver disease. Liver suffers from different type of diseases, like cirrhosis,

✉ R. V. Manjunath
manjunathrv@dsatm.edu.in

Anshul Ghanshala
anshulghanshala123@gmail.com

Karibasappa Kwadiki
KwadikiKaribasappa.cse@geu.ac.in

¹ Department of Electronics & Communication Engineering, Dayananda Sagar Academy of Technology and Management, Bangalore-82, India

² The Chinese University of Hong Kong, Hong Kong, SAR, China

³ Department of CS&IT, Graphic Era Deemed to be University, Dehradun 248002, India

hepatitis, liver cancer etc. [10]. Due to cirrhosis and liver cancer, there are around 50 million people who died worldwide every year from past two decades [22]. Cancer spreading from cancer affected organs of the body into the liver or vice versa called Metastatic cancer [19, 21]. The cancer cells that grow in liver metastasis are cells from part of the body where cancer is originated. Since the cancer is spread from other organ to liver doctor may diagnose it as progressive cancer or stage 4 cancer. Common types of cancer that spread to the liver are colorectal, lung, breast, pancreatic, stomach, esophagus, melanoma, etc. Where maximum people will develop metastasis on both lobes of the liver [19]. The cancer originated in the bile duct of the human is called cholangiocarcinoma. Cholangiocarcinoma is the second most common primary hepatobiliary tumour and recently it is increasing globally. Cholangiocarcinoma which is intrahepatic or extrahepatic also called as bileduct cancer as it is originated from the bileduct [6]. We have different types of liver diseases, in this work we are mainly focusing on Metastatic and cholangiocarcinoma cancer which are life threatening.

Automatic Identification and classification of these diseases will help in avoiding the manual diagnosis. In this paper we are developing an automatic model for binary classification of liver disease by comparing several classifiers such as machine learning and deep learning methods along with calculating confusion matrix to assess the classification using different metrics. One effective way to differentiate diseases from a given set of dataset is by means of feature extraction and selection. Feature extraction includes extracting texture, geometrical and statistical features. Texture analysis is the mathematical parameter computation from a two-dimensional images on pixels, whereas statistical and geometrical features are used in various medical recognition methods. Extracting different statistical, geometrical and texture features from a given set of datasets and selecting a particular feature to classify the disease can be done using a deep learning model. In several areas such as image classification, image recognition, speech recognition deep learning models are successfully used. Recently because of their feature selection and extraction capability, deep learning algorithms find a top place in biomedical applications [11]. These models become more powerful because models capable of learning features by themselves and they have high discriminatory power. A large quantity of manually labeled data from experts are required to develop a high-quality deep learning model, which is the main limitation of deep learning method. Due to patient privacy policy getting a large dataset in biomedical is a difficult task hence we have to develop an algorithm which learns features very quickly even for small datasets. The main contribution of this paper are as follows

- i) To develop an automatic deep learning model for detection and classification of liver disease
- ii) Preparing a labeled dataset with the help of expert radiologist from the 3Dircadb dataset and selecting the optimal features which improves the performance
- iii) Developing a confusion matrix to calculate different metrics.
- iv) Our developed method reached a dice score of 98.59%, an accuracy of 98.61% and a specificity of 100% on a labelled 3dircadb dataset

This paper is arranged as follows. Related work on identification and classification of liver diseases discussed in Section 2. Section 3 presents about explanation of dataset, proposed modified Unet-60 network architecture, feature extraction, feature selection.

Section 4 is about implementation, results and comparison with other works. Finally, Section 5 conclusion.

2 Literature review

Increasing access to hidden attributes in the medical dataset permit us to predict liver diseases using deep learning models. To predict liver diseases with good accuracy different datasets containing binary computed tomography images, histologically marked slide images, blood panels with liver tests, and molecular pointers present in blood samples have been used to train classifiers. In the following papers, recent studies related to liver disease identification and classification are introduced.

Dehua Chen et al. [5] developed a knowledge-powered deep breast tumor classification model using deep neural networks. The model is evaluated on a dataset containing 3.96 k patients data. Each patient is having four clinical reports of ultrasound, mammography, computed tomography and magnetic resonance imaging. The model can learn to extract features hierarchically and pay attention to important elements like words and sentences in the clinical reports. Proposed method achieved an accuracy of 0.8854, recall of 0.8771 and F1 score of 0.9070.

Ahmed Gaber et al. [9] developed a computer aided diagnosis method using machine learning and a voting-based classifier for ultrasound images to classify liver images as fatty or normal based on features extraction. Here to reduce the number of computations multi region of interest is selected and from each region of interest 26 features were extracted. The voting-based classifier achieved a classification accuracy of 95.71% which shows the strength of the model. The drawback of the work is limited dataset.

Mehdi Hosseinza et al. [12] proposed a diagnostic prediction model for chronic kidney diseases and its severity level that applies IOT multimedia data [26]. Different classification techniques are used to assess the chronic liver disease prediction and its level by selecting different features based on expert clinical observations and also earlier studies for chronic kidney diseases in various sets of multimedia datasets. By applying decision tree classifier on the prepared dataset with selected features produces an accuracy of 97%, sensitivity of 99% and specificity of 95% and also improves the execution time compared to other models.

Rayaan Azam Khan et al. [17] proposed a review paper which discuss about the computer aided diagnosis system for malignant liver detection and treatment and also discussed three image acquisition modalities like computed tomography, ultrasonography, and magnetic resonance imaging. Further preprocessing of images, extraction and selection of features also discussed with their pros and cons in addition to a lot of state of the art algorithms discussed which utilises numerous methodologies to fulfill the diagnostic tasks.

Mohammad Saber Iraj et al. [13] developed a method to detect covid-19 in X-ray images with the help of feature selection using deep convolutional neural network and binary differential algorithm. The database consists of three different categories of 1092 images including covid 19, pneumonia and healthy images. The method has achieved an accuracy of 0.9943, sensitivity of 0.9916 and specificity of 0.9957. Developed method can be applied in various medical applications.

Halgurd S. Maghdid et al. [20], developed a method for detecting coronavirus disease using alexnet model with convolutional neural network in computed tomographic and X-ray images. The dataset used for the detection of coronavirus is collected from different sources.

The experimental results obtained an accuracy of 0.98% using alexnet model whereas using updated convolutional network accuracy is settled at 0.94%.

Joel Jacob et al. [14] proposed a diagnosis of liver disease using machine learning techniques. He utilised Indian liver patient dataset comprising ten diverse attributes of 583 patients by using distinct algorithms like Logistic regression, K nearest neighbour, support vector machine, & artificial neural network which produced 0.7323, 0.7205, 0.7504 & 0.928 accuracy correspondingly.

Joloudari J. H et al. [16] proposed a method using hybrid support vector machine with particle swarm optimization which achieved a maximum accuracy over support vector machine, random forest, Bayesian network, multilayer perceptron, and a neural network for the liver disease detection by predicting maximum number of features. The accuracy was calculated as 0.8735, 0.7891, 0.6678, 0.7651 and 0.9517 for random forest, multilayer perceptron, neural network, support vector machine and pso-svm models. Here hybrid pso-svm achieved a highest accuracy with least number of selected features.

Keerthana Jagnathan et al. [15] using support vector machine and optimal descriptor sets proposed a prediction of drug induced liver toxicity. By using machine learning quantitative structure activity relationship models are constructed and for molecular descriptors sets feature selection methods are constructed. Here different feature selection methods are used to improve the prediction performance. Experimental results showed that with reduced number of molecular descriptors support vector machine classifier developed a better classification accuracy.

Phan and Chan et al. [25] proposed a deep learning model to detect liver cancer in hepatitis patients and this model achieved an accuracy of 0.98% with convolutional neural network in identifying the liver cancer. To distinguish health signals from the disease history in the hepatitis cohort which in turn predicts liver cancer. The state of art techniques applied through deep learning methods. When analysed by age the hepatitis is increased in older groups compared to any other age group and in future these deep learning methods are applied on identifying severe diseases.

Abhay Krishnan et al. [18] developed a multi-level ensemble model to detect and classify liver cancers such as hepatocellular carcinoma, which works on feature extraction. To explain the robustness of the classifiers K-fold cross validation is also used. This model achieved a maximum accuracy in the detection and classification of different tumors compared to diverse classifiers.

Yu Sub Sung et al. [29] proposed radiomics and deep learning in liver disease combination used in various liver imaging fields such as liver fibrosis, prognosis of malign tumors, automated detection and characterisation of liver tumors, abdominal organ segmentation and body composition analysis. This study aimed at anticipate binary classifications of liver disease by comparing among several classifiers, machine learning and deep learning methods and also to calculate confusion matrices for comparing target classes with output classes.

3 Methods

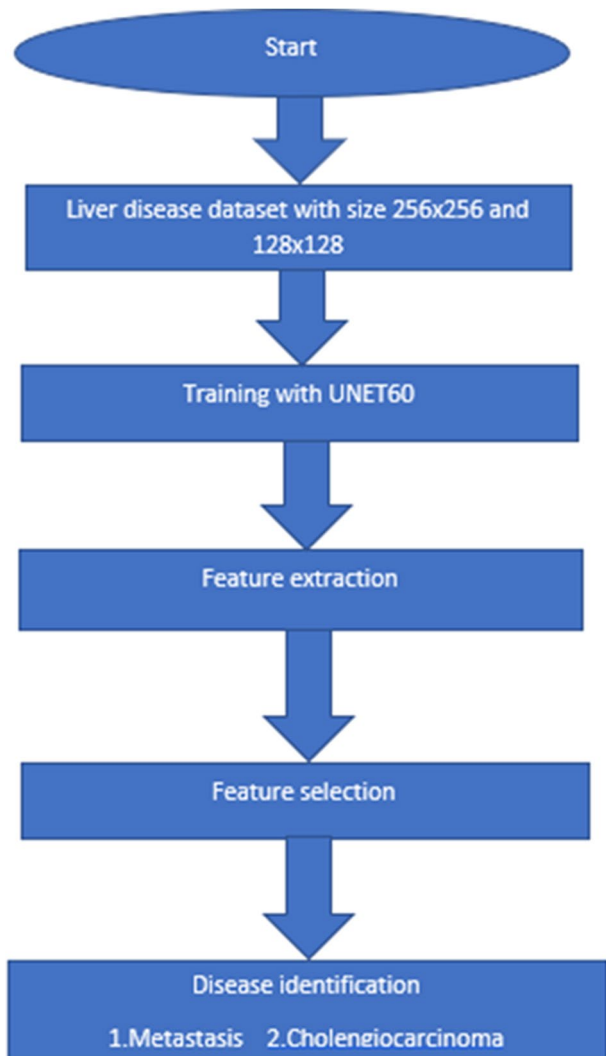
We proposed a deep learning model called modified Unet 60 for detection and classification of liver diseases from a given set of datasets. The proposed workflow for identification and classification of liver diseases is presented in Fig. 1. Liver disease CT images has been trained using Unet-60 deep learning model. The excerpted statistical, textural

and geometrical features were used to select and classify the Metastasis and cholangiocarcinoma tumors.

3.1 Dataset

Overall, with data augmentation 864 liver cancer images collected from 3Dircadb publicly available dataset. Among the 864 images, 360 images belong to Metastasis cancer and remaining 360 images belongs to Cholangiocarcinoma, here around 720 CT images are used for training and 144 CT images for testing. Labelling of CT images for entire dataset containing 20 CT volumes is done by a well-known radiologist. Here the CT images are resized to size 256×256 and 128×128 from 512×512 due to limited CPU using MATLAB tool.

Fig. 1 Flow of the planned system



3.2 Grouped data

By converting the images from dicom to jpg and png format, and removing the images with no liver and tumor among labelled data, the deep learning model is trained and tested on these CT images. In the 3Dircadb dataset we have a separate mask for both liver and its tumor.

3.3 Network architecture

Signifying the traditional deep convolutional neural network here we developed a modified Unet 60 model for the detection and classification of liver diseases. The network architecture is based on the original UNET architecture, however the novelty of the paper is the model itself which is designed using 60 layers without a batchnormalisation layer which is important for normalizing the outputs of convolutional layers, and a maxpool layer is included after every pair of convolutional and relu layers in the expansion path along with one dropout layer at the end of the encoder path which deactivates some of the neurons to control overfitting of the network. Other modifications are done on filters at each convolutional block where 32 filters are present in the first block and it will be doubled for the consecutive three blocks and becomes 256 at the last convolutional block. At the end of the contraction path a globalmaxpooling layer is included. Left hand side of the network is called as encoder which is used for framework seizure, which consist of 8 pairs of convolutional and relu layers, 3 maxpooling layers and at the end one dropout layer whereas right hand side of the network is called as decoder which contains 8 pairs of convolutional and relu layers and 4 layers of upconvolution and uprelu which is used for highlighting the specific position, finally encoder and decoder connected using bridge network with the help of 4 depth concatenation layers. The entire structure is in the form of letter U hence the name is given as Unet. By increasing the number of hidden layers inside the network performance can be endorsed. The architecture of the proposed model is shown in Fig. 2. Binary CT labelled dataset is passed through a Unet 60 model which is trained by tuning different hyper parameters. The Unet60 model extracts features from the binary CT images. On these extracted features binary differential evolution algorithm is applied to select best features suitable for classification. Using the selected best features the classification of Liver disease using CT images has been performed and their classification is assessed by different metrics. Different layers used in the proposed model is explained below and also analysis of the model is shown in Fig. 3.

Convolutional layer It contains a filter with size 3×3 that convolves around the input image. By performing a dot product operation between the filter weight content and every location of the image outcome of the layer is attained.

Relu layer It is an activation function, which sets negative values to zero in a matrix. It performs a threshold operation to each element of the input.

Maxpool layer Its nature is similar to that of convolutional layer. It is applied on every individual location in the input image which takes maximum neighbouring value. It is used to reduce the spatial size in the middle of the architecture.

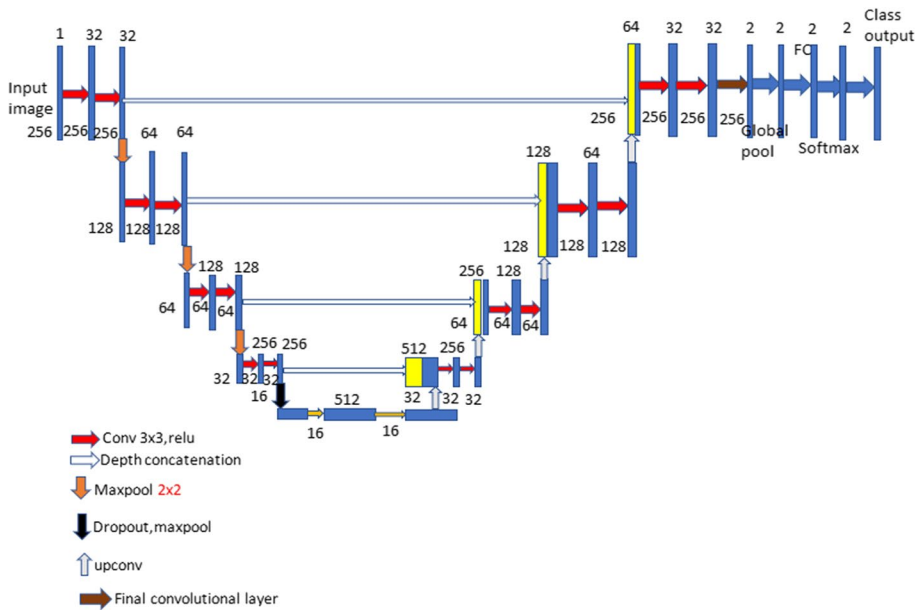


Fig. 2 Modified UNET-60 architecture

Dropout layer The dropout layer reduces the overfitting in the model, and it acts as a mask that removes some neurons contributions to the succeeding layer while leaving all others unchanged. Here we set dropout layer value to 0.5.

Depth concatenation layer It is a layer used to transfer the features of the encoder to the decoder.

Up convolutional layer A transposed convolutional layer used for up sampling that is to generate an output feature map that has a spatial dimension greater than that of the input feature map.

Global pool layer To review the presence of a feature in an image global pool layer is used in the model. It can also be used as an alternative for fully connected layer which act as an output predictor.

Fully connected layer It is used at the end of the model which act as a output predictor. Here each neuron is fully connected to every other neuron in the previous layer. It uses features learned by previous layers to make decisions.

Softmax layer It is applied at the end of the model which will serve as a classifier and it is responsible for categorizing different inputs into distinct types.

Classification output layer This layer computes the cross-entropy loss for classification and weighted classification tasks with mutually exclusive classes.

ANALYSIS RESULT						
#	Name	Type	Activations	Learnables	Total Learnab...	States
1	ImageInputLayer 128x128x1 images with zero-center normalization	Image Input	128x128x1	-		0 -
2	Encoder-Stage-1-Conv-1 32 3x3x1 convolutions with stride [1 1] and padding 'same'	Convolution	128x128x32	Weights 3x3x1x32 Bias 1x1x32	320	-
3	Encoder-Stage-1-ReLU-1 ReLU	ReLU	128x128x32	-		0 -
4	Encoder-Stage-1-Conv-2 32 3x3x2 convolutions with stride [1 1] and padding 'same'	Convolution	128x128x32	Weights 3x3x2x32 Bias 1x1x32	9248	-
5	Encoder-Stage-1-ReLU-2 ReLU	ReLU	128x128x32	-		0 -
6	Encoder-Stage-1-MaxPool 2x2 max pooling with stride [2 2] and padding [0 0 0 0]	Max Pooling	64x64x32	-		0 -
7	Encoder-Stage-2-Conv-1 64 3x3x2 convolutions with stride [1 1] and padding 'same'	Convolution	64x64x64	Weights 3x3x2x64 Bias 1x1x64	18496	-
8	Encoder-Stage-2-ReLU-1 ReLU	ReLU	64x64x64	-		0 -
9	Encoder-Stage-2-Conv-2 64 3x3x4 convolutions with stride [1 1] and padding 'same'	Convolution	64x64x64	Weights 3x3x4x64 Bias 1x1x64	36928	-
10	Encoder-Stage-2-ReLU-2 ReLU	ReLU	64x64x64	-		0 -
11	Encoder-Stage-2-MaxPool 2x2 max pooling with stride [2 2] and padding [0 0 0 0]	Max Pooling	32x32x64	-		0 -
12	Encoder-Stage-3-Conv-1 128 3x3x4 convolutions with stride [1 1] and padding 'same'	Convolution	32x32x128	Weights 3x3x4x128 Bias 1x1x128	73856	-
13	Encoder-Stage-3-ReLU-1 ReLU	ReLU	32x32x128	-		0 -
14	Encoder-Stage-3-Conv-2 128 3x3x12 convolutions with stride [1 1] and padding 'same'	Convolution	32x32x128	Weights 3x3x12x128 Bias 1x1x128	147584	-
15	Encoder-Stage-3-ReLU-2 ReLU	ReLU	32x32x128	-		0 -
16	Encoder-Stage-3-MaxPool 2x2 max pooling with stride [2 2] and padding [0 0 0 0]	Max Pooling	16x16x128	-		0 -
17	Encoder-Stage-4-Conv-1 256 3x3x12 convolutions with stride [1 1] and padding 'same'	Convolution	16x16x256	Weights 3x3x12x256 Bias 1x1x256	295168	-
18	Encoder-Stage-4-ReLU-1 ReLU	ReLU	16x16x256	-		0 -
19	Encoder-Stage-4-Conv-2 256 3x3x256 convolutions with stride [1 1] and padding 'same'	Convolution	16x16x256	Weights 3x3x256x256 Bias 1x1x256	590080	-
20	Encoder-Stage-4-ReLU-2 ReLU	ReLU	16x16x256	-		0 -
21	Encoder-Stage-4-DropOut 50% dropout	Dropout	16x16x256	-		0 -
22	Encoder-Stage-4-MaxPool 2x2 max pooling with stride [2 2] and padding [0 0 0 0]	Max Pooling	8x8x256	-		0 -
23	Bridge-Conv-1 512 3x3x256 convolutions with stride [1 1] and padding 'same'	Convolution	8x8x512	Weights 3x3x256x512 Bias 1x1x512	1189160	-
24	Bridge-ReLU-1 ReLU	ReLU	8x8x512	-		0 -
25	Bridge-Conv-2 512 3x3x12 convolutions with stride [1 1] and padding 'same'	Convolution	8x8x512	Weights 3x3x512x512 Bias 1x1x512	2359808	-
26	Bridge-ReLU-2 ReLU	ReLU	8x8x512	-		0 -
27	Bridge-DropOut 50% dropout	Dropout	8x8x512	-		0 -
28	Decoder-Stage-1-UpConv 256 2x2x512 transposed convolutions with stride [2 2] and or...	Transposed Convolution	16x16x256	Weights 2x2x256x512 Bias 1x1x256	524544	-
29	Decoder-Stage-1-UpReLU ReLU	ReLU	16x16x256	-		0 -
30	Decoder-Stage-1-DepthConcatenation Depth concatenation of 2 inputs	Depth concatenation	16x16x512	-		0 -
31	Decoder-Stage-1-Conv-1 256 3x3x512 convolutions with stride [1 1] and padding 'same'	Convolution	16x16x256	Weights 3x3x512x256 Bias 1x1x256	1179904	-
32	Decoder-Stage-1-ReLU-1 ReLU	ReLU	16x16x256	-		0 -

Fig. 3 Analysis of Unet 60

33	Decoder-Stage-1-Conv-2 256 3x3x256 convolutions with stride [1 1] and padding 'same'	Convolution	16x16x256	Weights 3x3x256x256 Bias 1x1x256	590880	-
34	Decoder-Stage-1-ReLU-2 ReLU	ReLU	16x16x256	-	0	-
35	Decoder-Stage-2-UpConv 128 2x2x256 transposed convolutions with stride [2 2] and cr...	Transposed Convol...	32x32x128	Weights 2x2x128x256 Bias 1x1x128	131200	-
36	Decoder-Stage-2-UpReLU ReLU	ReLU	32x32x128	-	0	-
37	Decoder-Stage-2-DepthConcatenation Depth concatenation of 2 inputs	Depth concatenation	32x32x256	-	0	-
38	Decoder-Stage-2-Conv-1 128 3x3x256 convolutions with stride [1 1] and padding 'same'	Convolution	32x32x128	Weights 3x3x256x128 Bias 1x1x128	295040	-
39	Decoder-Stage-2-ReLU-1 ReLU	ReLU	32x32x128	-	0	-
40	Decoder-Stage-2-Conv-2 128 3x3x128 convolutions with stride [1 1] and padding 'same'	Convolution	32x32x128	Weights 3x3x128x128 Bias 1x1x128	147584	-
41	Decoder-Stage-2-ReLU-2 ReLU	ReLU	32x32x128	-	0	-
42	Decoder-Stage-3-UpConv 64 8x8x128 transposed convolutions with stride [2 2] and cro...	Transposed Convol...	64x64x64	Weights 2x2x64x128 Bias 1x1x64	32032	-
43	Decoder-Stage-3-UpReLU ReLU	ReLU	64x64x64	-	0	-
44	Decoder-Stage-3-DepthConcatenation Depth concatenation of 2 inputs	Depth concatenation	64x64x128	-	0	-
45	Decoder-Stage-3-Conv-1 64 3x3x128 convolutions with stride [1 1] and padding 'same'	Convolution	64x64x64	Weights 3x3x128x64 Bias 1x1x64	73792	-
46	Decoder-Stage-3-ReLU-1 ReLU	ReLU	64x64x64	-	0	-
47	Decoder-Stage-3-Conv-2 64 3x3x64 convolutions with stride [1 1] and padding 'same'	Convolution	64x64x64	Weights 3x3x64x64 Bias 1x1x64	36928	-
48	Decoder-Stage-3-ReLU-2 ReLU	ReLU	64x64x64	-	0	-
49	Decoder-Stage-4-UpConv 32 2x2x64 transposed convolutions with stride [2 2] and crop...	Transposed Convol...	128x128x32	Weights 2x2x32x64 Bias 1x1x32	8124	-
50	Decoder-Stage-4-UpReLU ReLU	ReLU	128x128x32	-	0	-
51	Decoder-Stage-4-DepthConcatenation Depth concatenation of 2 inputs	Depth concatenation	128x128x64	-	0	-
52	Decoder-Stage-4-Conv-1 32 3x3x64 convolutions with stride [1 1] and padding 'same'	Convolution	128x128x32	Weights 3x3x64x32 Bias 1x1x32	18464	-
53	Decoder-Stage-4-ReLU-1 ReLU	ReLU	128x128x32	-	0	-
54	Decoder-Stage-4-Conv-2 32 3x3x32 convolutions with stride [1 1] and padding 'same'	Convolution	128x128x32	Weights 3x3x32x32 Bias 1x1x32	9248	-
55	Decoder-Stage-4-ReLU-2 ReLU	ReLU	128x128x32	-	0	-
56	Final-ConvolutionLayer 2 3x3x2 convolutions with stride [1 1] and padding 'same'	Convolution	128x128x2	Weights 3x3x32x2 Bias 1x1x2	578	-
57	globalpool Global max pooling	Global Max Pooling	1x1x2	-	0	-
58	fc 2 fully connected layer	Fully Connected	1x1x2	Weights 2x2 Bias 2x1	6	-
59	softmax-Layer softmax	Softmax	1x1x2	-	0	-
60	classOutput crossentropyk	Classification Output	-	-	0	-

Fig. 3 (continued)

3.4 Feature extraction

Feature extraction is one of the significant parts in the classification of liver diseases since it identifies the essential details about the contents of an image [27, 28]. The Unet 60 model is capable of extracting statistical features from the binary CT images such as shape, size, area and total number of connected components etc. Among the extracted features, best features are selected using feature selection method for the liver disease classification.

3.5 Feature selection

For precise liver disease classification all the extracted features that influence on liver disease classification is included [12]. A Binary differential evolution algorithm is a feature

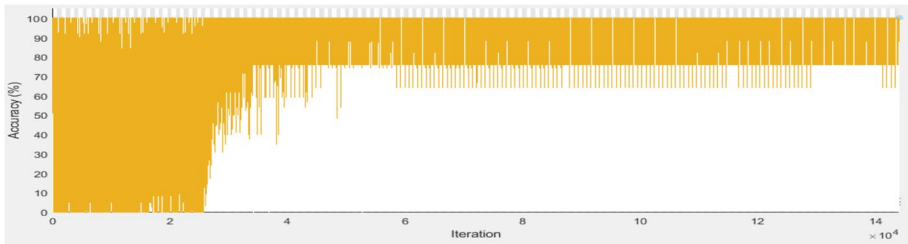


Fig. 4 Accuracy vs Iterations

selection method used to select a relevant feature by eliminating unrelated features [13]. Feature selection is generally applied

- i) To minimize the number of features
- ii) To minimize the computational cost
- iii) To reduce the features which reduce the storage requirement

Features like area, mass, number of connected components, correlation, size are selected from the dataset to classify the liver diseases.

4 Results and discussion

The proposed system for liver cancer detection and classification is trained and tested on 864 CT images containing cancer lesions. The developed model utilizes resultant binary segmented tumors from Unet architecture or CT images from the 3Dircadb dataset (<https://www.ircad.fr/research/data-sets/liver-segmentation-3d-ircadb-01/>). The Unet 60 model with different layers performs feature extraction and suitable extracted features are selected using feature selection method to identify and classify liver diseases.

4.1 Metrics for evaluation

At the authentication phase, parameters like accuracy, sensitivity, specificity, dice similarity coefficient, True positive, True negative, False positive, False negative are used to check

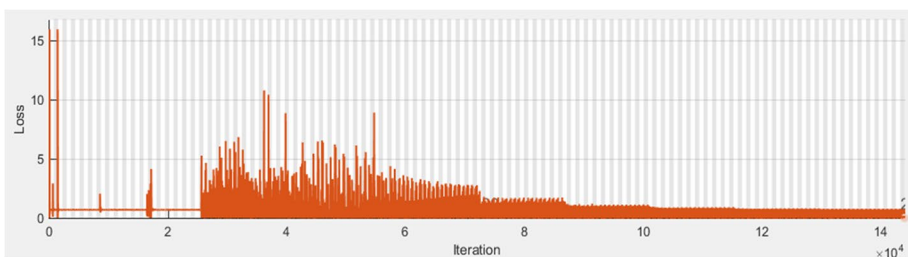


Fig. 5 Loss vs Iterations

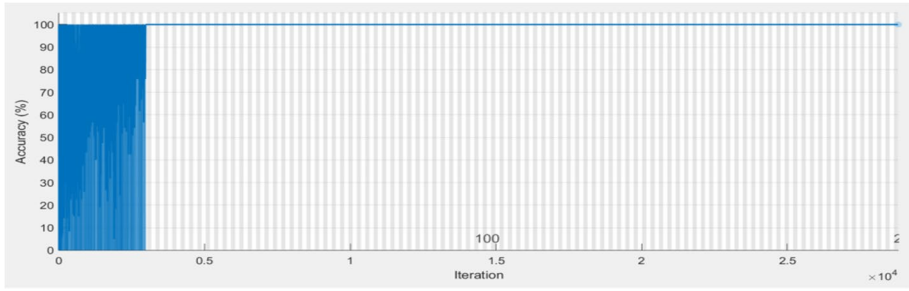


Fig. 6 Accuracy vs Iterations

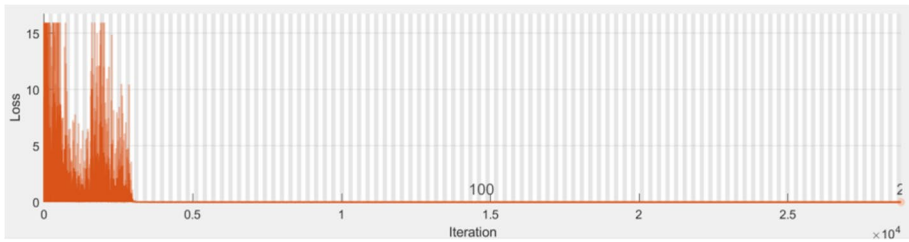


Fig. 7 Loss vs Iterations

the attainment of the deep learning model. The equations of the above parameters are specified below with explanation.

- (1) Accuracy [31]: It is the ratio of correct number of identified pixels to the total number of pixels in an image.

$$\text{Accuracy} = \frac{TP + TN}{TP + TN + FP + FN} \tag{1}$$

- (2) Sensitivity [31]: It is the measure of actual positive values percentage which are correctly identified.

$$\text{Sensitivity} = \frac{TP}{TP + FN} \tag{2}$$

Table 1 Confusion Matrix details for training

Training set		
Class	Cholangiocarcinoma	Metastasis carcinoma
Cholangiocarcinoma	356	2
Metastasis carcinoma	4	358

Table 2 Confusion Matrix details for testing

Testing set		
Class	Cholangiocarcinoma	Metastasis carcinoma
Cholangiocarcinoma	70	0
Metastasis carcinoma	2	72

(3) Specificity [31]: It is the measure of actual negative values percentage which are correctly identified.

$$\text{Specificity} = \frac{TN}{TN + FP} \tag{3}$$

(4) Dice score [1, 3]: It is a measure of till what degree of extent both the samples are similar.

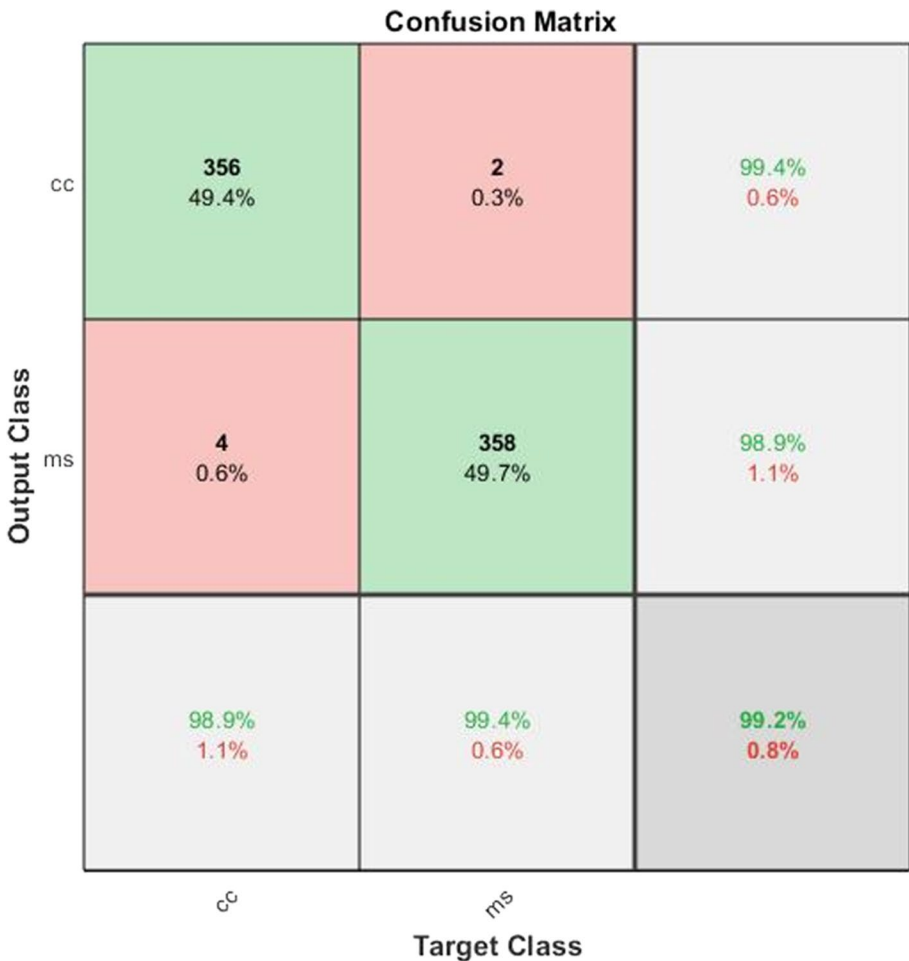


Fig. 8 Confusion matrix for training

$$\text{Dice} = \frac{2TP}{2TP + FP + FN} \tag{4}$$

4.2 Implementation and testing assessment

The developed technique was trained on a desktop computer with a MATLAB 2020a tool using adam optimizer with a learning rate of 0.001, learn rate drop factor of 0.5, minibatch size of one, learn rate is piecewise, learn rate drop period of 20 and these parameter values are derived from repeated training. Randomly from the dataset 85% were used for training and 15% were used for testing. By utilizing 60 layers from the network, model trained for 200 epochs where each epoch took 720 iterations leading to a total of 144,000 iterations. The training progress of the model with respect to the accuracy, loss vs iterations is shown in Figs. 4 and 5 respectively whereas Figs. 6 and 7 represents the graph of testing data. From the Figs. 4 and 6 it is clear that as the number of iterations increases the loss decreases gradually and remains constant after certain iterations, whereas in Figs. 5 and 7 accuracy of the model increases after certain iterations and remains constant till the end of training and testing.

Classification results Classification of Metastasis carcinoma and cholangiocarcinoma can be achieved using the proposed modified Unet 60. The confusion matrix for training and

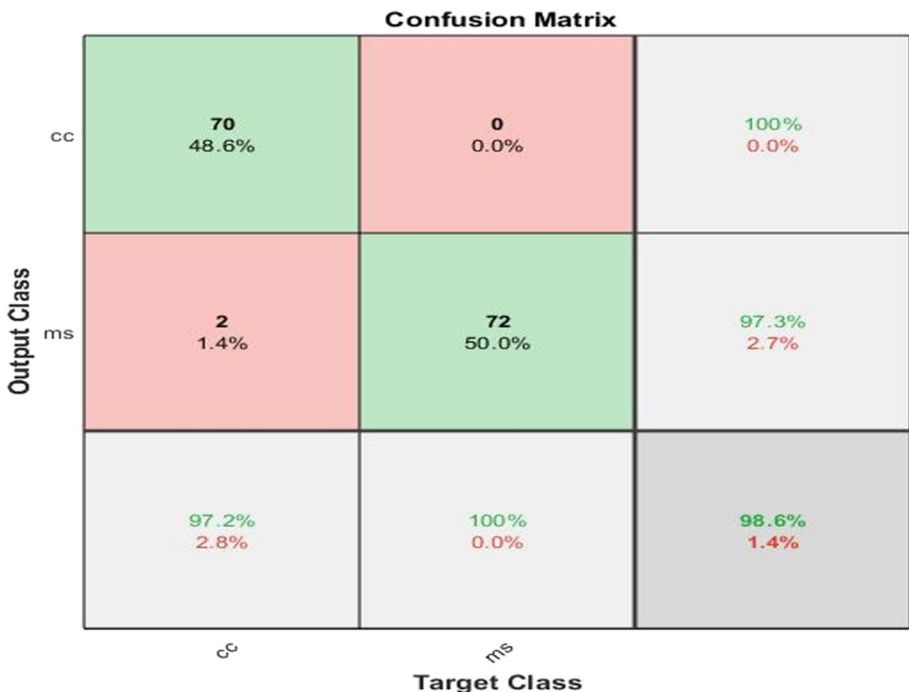


Fig. 9 Confusion matrix for testing


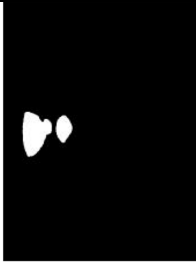
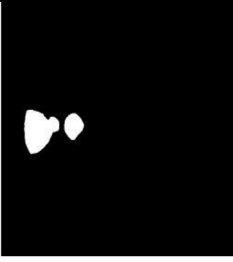



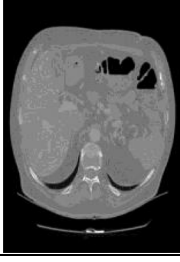

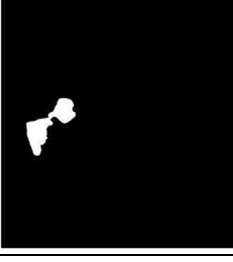
Si nos	Input CT	Ground truth image	Metastasis carcinoma segmented
1			
2			
3			

Fig. 10 Results of the metastatic carcinoma

testing data is shown in Tables 1 and 2. Table 1 contains resultant data where classifier correctly predicts 356 cholangiocarcinoma and 358 metastasis carcinoma images out of total 720 images. Whereas Table 2 displays data related to testing of 144 images in which classifier able to predict correctly 70 images of cholangiocarcinoma and 72 images of metastatic carcinoma. The confusion matrix for both training and testing data is shown in Figs. 8 and 9 respectively where it is displaying an accuracy of 99.2% with 0.8% loss for training data and an accuracy of 98.6% with 1.4% loss for testing data. The results of the proposed model are shown in Figs. 10 and 11 correspondingly. Table 3 shows the results obtained for different metrics for testing the dataset using trained model. We have compared our model results with different classifiers and a summary of the comparison is displayed in Table 4. From Table 4 we observed that the proposed method has better accuracy, dice similarity coefficient, and specificity compared to other models as we increase the number of test samples accuracy of the model also increases, this we can conclude from the training dataset as it achieves an accuracy of 99.2% in training.

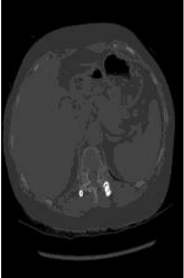
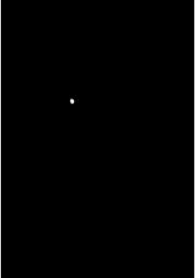

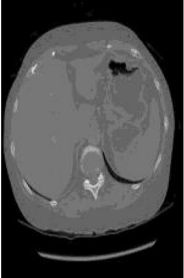
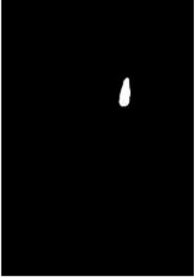

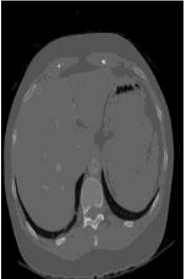

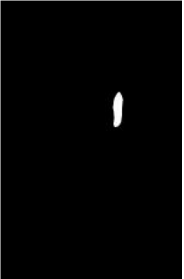
Si nos	Input CT	Ground truth image	Cholangiocar-cinoma segmented
1			
2			
3			

Fig. 11 Results of the cholangiocarcinoma

As shown below in Fig. 10, first column represents original CT images, second column indicates the original masks of the liver tumor taken for training, third column indicates results of detected and classified metastasis carcinoma images.

Table 3 Results obtained for the proposed model

Parameters	Testing dataset
Accuracy	98.61
sensitivity	97.22
specificity	100
DSC	98.59

Table 4 Different classifiers comparison

Classifiers	Accuracy (%)	Specificity (%)	Sensitivity (%)	DSC (%)
MLP [7]	91.65	93.08	89.58	–
ADABOOST M1 [7]	90.72	92.47	87.97	–
SVM [7]	95.17	95.76	94.22	–
KNN [7]	93.87	95.31	92.56	–
NAÏVE BAYES [7]	91.94	93.65	89.91	–
RANDOM FOREST [7]	94.86	95.38	93.88	–
DNN [7]	98.38	99.09	100	–
ANN [23]	88.89	82.88	95.23	–
MLP [8]	89.15	88.01	90.38	89.05
C4.5 [8]	95.02	96.12	93.89	94.41
CNN [30]	88.00	–	–	–
CNN [8]	96.00	–	–	–
CNN [2]	89.58	–	–	–
CNN [24]	86.90	–	–	–
KNN, SVM, RF [4]	96.60	–	–	–
PROPOSED MODEL	98.61	100	97.22	98.59

As shown below in Fig. 11, first column displays original CT images, second column displays the original masks of the liver tumor taken for training, third column indicates results of detected and classified cholangiocarcinoma images.

5 Conclusions and future work

Here we have developed a deep learning classifier to detect and classify two different liver diseases. The diagnostic performance of the modified Unet-60 is superior to other identified classifiers as it has achieved a high accuracy of 98.61%, sensitivity of 97.22%, 100% of specificity, and importantly it achieved a dice score of **98.59%** which is superior compared to any classifier. In the future, we would like to work on reducing the time taken by the developed model to train the dataset, and also a greater number of labeled CT images with different liver diseases need to be investigated. Further disease identification must be investigated through 3D-volumetric analysis of a liver. As a substitute for binary classification, we can practice multinominal classification by differentiating the liver disease types.

Data availability The datasets generated during and/or analysed during the current study are available from the corresponding author on reasonable request.

Declarations

Ethics approval and consent to participate We comply to the ethical standards. We give our consent to participate.

Consent for publication All the authors are giving consent to publish.

Informed consent Not applicable.

Research involving human participation and/or animals Not applicable.

Competing interests No conflict of interest to declare.

Conflict of interest The authors declare no conflict of interest, financial or otherwise.

References

1. Ahmad M et al (2019) Deep belief network modeling for automatic liver segmentation. *IEEE Access* 7:20585–20595
2. Balagourouchetty L, Pragatheeswaran JK, Pottakkat B, Ramkumar G (2020) GoogLeNet-based ensemble FCNet classifier for focal liver lesion diagnosis. *IEEE J Biomed Health Inform* 24(6):1686–1694. <https://doi.org/10.1109/JBHI.2019.2942774>
3. Bevilacqua V et al (2017) A novel approach for hepatocellular carcinoma detection and classification based on triphasic CT protocol. In: A novel approach for hepatocellular carcinoma detection and classification based on triphasic CT protocol, pp 1856–1863
4. Bharti P, Mittal D, Ananthasivan R (2018) Preliminary study of chronic liver classification on ultrasound images using an ensemble model. *Ultrason Imaging* 40(6):357–379. <https://doi.org/10.1177/0161734618787447>
5. Chen D, Huang M, Li W (2019) Knowledge-powered deep breast tumor classification with multiple medical reports. *IEEE/ACM Trans Comput Biol Bioinform* 18(3):891–901
6. Cholangiocarcinoma cancer. Available online: <https://radiopaedia.org/articles/cholangiocarcinoma>. Accessed on 10 Dec 2021
7. Das A, Rajendra Acharya U, Panda SS, Sabut S (2018) Deep learning based liver cancer detection using watershed transform and Gaussian mixture model techniques. *Cogn Syst Res*. <https://doi.org/10.1016/j.cogsys.2018.12.009>
8. Das A, Das P, Panda SS, Sabut S (2019) Detection of liver cancer using modified fuzzy clustering and decision tree classifier in CT images. *Pattern Recognit Image Anal* 29(2):201–211. <https://doi.org/10.1134/S1054661819020056>
9. Gaber A, Youness HA, Hamdy A, Abdelaal HM, Hassan AM (2022) Automatic classification of fatty liver disease based on supervised learning and genetic algorithm. *Appl Sci* 12:521. <https://doi.org/10.3390/app12010521>
10. Gatos I, Tsantis S, Spiliopoulos S, Karnabatidis D, Theotokas I, Zoumpoulis P, Loupas T, Hazle JD, Kagadis GC (2017) A machine-learning algorithm toward color analysis for chronic liver disease classification, employing ultrasound shear wave elastography. *Ultrasound Med Biol* 43:1797–1810
11. Gogate M, Dashtipour K, Bell P, Hussain A (2020) Deep neural network driven bi-natural audio-visual speech separation. In: Proceedings of the 2020 International Joint Conference on Neural Networks (IJCNN), Glasgow, pp 1–7
12. Hosseinzadeh M, Koohpavehkhadeh J, Bali AO, Asghari P, Soury A, Mazaherinezhad A, Bolouli M, Rawassizadeh R (2021) A diagnostic prediction model for chronic kidney disease in internet of things platform. *Multimed Tools Appl* 80:16933–16950. <https://doi.org/10.1007/s11042-020-09409-4>
13. Irajy MS, Derakhshi MRF, Tanha J (2021) Covid-19 detection using deep convolutional neural networks and binary differential algorithms based feature selection from X-ray images. *Hindawi complexity* 2021:9973277. <https://doi.org/10.1155/2021/9973277>
14. Jacob J, Mathew JC, Mathew J, Issac E (2018) Diagnosis of liver disease using machine learning techniques. *Int Res J Eng Technol* 5(04)
15. Jaganathan K, Tayara H, Chong KT (2021) Prediction of drug-induced liver toxicity using SVM and optimal descriptor sets. *Int J Mol Sci* 22:8073
16. Joloudari JH, Saadatfar H, Dehzangi A, Shamshirband S (2019) Computer-aided decision-making for predicting liver disease using PSO-based optimized SVM with feature selection. *Inform Med Unlocked* 17:100255
17. Kahn RA, Luo Y, Wu F-X (2022) Machine learning based liver disease diagnosis: a systematic review. *Neurocomputing* 468:492–509. <https://doi.org/10.1016/j.neucom.2021.08.138>

18. Krishnan A, Mittal D (2021) Ensembled liver cancer detection and classification using CT images. *Proc Inst Mech Eng H* 235(2):232–244
19. Liver Metastasis. Available online: <https://www.healthline.com/health/liver-metastases>. Accessed on 14 Dec 2018
20. Maghdid HS, Asaad AT, Ghafoor KZ, Sadiq AS, Khan MK (2020) Diagnosing COVID-19 pneumonia from X-Ray and CT images using deep learning and transfer learning algorithms. *arXiv preprint arXiv:2004.00038*
21. Metastatic Cancer. Available online: <http://www.cancer.ca/en/cancerinformation/cancer-type/metastatic-cancer/liver-metastases/?region=on>. Accessed on 10 December 2021
22. Miriam E (2013) Tucker The Liver Meeting 2013: American Association for the Study of Liver Diseases (AASLD). *Medscape*. Available online: <https://www.medscape.com/viewarticle/813788>. Accessed on 14 Dec 2018
23. Mostafa F, Hasan E, Williamson M, Khan H (2021) Statistical machine learning approaches to liver disease prediction. *Livers* 1:294–312
24. Muthuswamy J (2019) Extraction and classification of liver abnormality based on neutrosophic and SVM classifier. In: *Progress in advanced computing and intelligent engineering*. Springer, pp 269–279. <https://doi.org/10.1007/978-981-13-1708-825.24>
25. Phan DV, Chan CL, Li AA, Chien TY, Nguyen VC (2020) Liver cancer prediction in a viral hepatitis cohort: a deep learning approach. *Int J Cancer* 147:2871–2878
26. Rahamani AM, Babaei Z, Soury A (2021) Event-driven IoT architecture for data analysis of reliable healthcare application using complex event processing. *Clust Comput* 24:1347–1360, Springer. <https://doi.org/10.1007/s10586-020-03189-w>
27. Rajathi GI, Jiji GW (2019) Chronic liver disease classification using hybrid whale optimisation with simulated annealing and ensemble classifier. *Symmetry* 11:33. <https://doi.org/10.3390/sym11010033>
28. Renukadevi NT (2021) Performance evaluation of hybrid machine learning algorithms for medical image classification. *Advanced soft computing techniques in data science, IoT and cloud computing, studies in big data volume 89*. Springer, Cham. https://doi.org/10.1007/978-3-030-75657-4_12
29. Sung YS, Park B, Park HJ, Lee SS (2021) Radiomics and deep learning in liver diseases. *J Gastroenterol Hepatol* 36:561–568
30. Yamakawa M, Shiina T, Nishida N, Kudo M (2019) Computer aided diagnosis system developed for ultrasound diagnosis of liver lesions using deep learning. *IEEE International Ultrasonics Symposium, IUS 2019-October*, pp 2330–2333. <https://doi.org/10.1109/ULTSYM.2019.8925698.21>
31. Zhang T, Zhang S, Jin C et al (2021) A predictive model based on the gut microbiota improves the diagnostic effect in patients with Cholangiocarcinoma. *Front Cell Infect Microbiol*. <https://doi.org/10.3389/fcimb.2021.751795>

Publisher's note Springer Nature remains neutral with regard to jurisdictional claims in published maps and institutional affiliations.

Springer Nature or its licensor (e.g. a society or other partner) holds exclusive rights to this article under a publishing agreement with the author(s) or other rightsholder(s); author self-archiving of the accepted manuscript version of this article is solely governed by the terms of such publishing agreement and applicable law.